Transmembrane Extension and Oligomerization of the CLIC1 Chloride Intracellular Channel Protein upon Membrane Interaction

5 AUTHORS, INCLUDING:

Sophia C Goodchild
University of New South Wales
12 PUBLICATIONS **128** CITATIONS

SEE PROFILE

Christopher Angstmann
University of New South Wales
25 PUBLICATIONS **57** CITATIONS

SEE PROFILE

Louise J Brown
Macquarie University
57 PUBLICATIONS **1,010** CITATIONS

SEE PROFILE

Transmembrane Extension and Oligomerization of the CLIC1 Chloride Intracellular Channel Protein upon Membrane Interaction

Sophia C. Goodchild,[†] Christopher N. Angstmann,[‡] Samuel N. Breit,[§] Paul M. G. Curmi,[§,⊥] and Louise J. Brown*,[†]

[†]Department of Chemistry and Biomolecular Sciences, Macquarie University, Sydney, New South Wales 2109, Australia
[‡]School of Mathematics and Statistics, University of New South Wales, New South Wales 2052, Australia
[§]St. Vincent's Centre for Applied Medical Research, St. Vincent's Hospital, Sydney, NSW 2010, Australia
[⊥]School of Physics, University of New South Wales, New South Wales 2052, Australia

S Supporting Information

ABSTRACT: Chloride intracellular channel proteins (CLICs) differ from most ion channels as they can exist in both soluble and integral membrane forms. The CLICs are expressed as soluble proteins but can reversibly autoinsert into the membrane to form active ion channels. For CLIC1, the interaction with the lipid bilayer is enhanced under oxidative conditions. At present, little evidence is available characterizing the structure of the putative oligomeric CLIC integral membrane form. Previously, fluorescence resonance energy transfer (FRET) was used to monitor and model the conformational transition within CLIC1 as it interacts with the membrane bilayer. These results revealed a large-scale unfolding between the C- and N-domains of CLIC1 as it interacts with the membrane. In the present study, FRET was used to probe lipid-induced structural changes arising in the vicinity of the putative transmembrane region of CLIC1 (residues 24−46) under oxidative conditions. Intramolecular FRET distances are consistent with the model in which the N-terminal domain inserts into the bilayer as an extended α-helix. Further, intermolecular FRET was performed between fluorescently labeled CLIC1 monomers within membranes. The intermolecular FRET shows that CLIC1 forms oligomers upon oxidation in the presence of the membranes. Fitting the data to symmetric oligomer models of the CLIC1 transmembrane form indicates that the structure is large and most consistent with a model comprising approximately six to eight subunits.
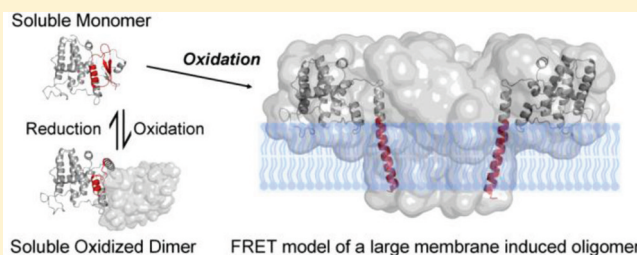
The chloride intracellular channels (CLICs) are a class of ubiquitously expressed anion channels possessing both enigmatic structural and functional properties. CLICs differ from classical ion channels as they are expressed as soluble proteins and lack both a leader sequence for membrane targeting and the multiple hydrophobic transmembrane domains, typical of classical ion channel proteins.[1] The CLIC proteins can undergo autonomous membrane insertion to form integral membrane ion channels.[2] Because of their ability to reversibly interconvert between multiple functional structures using the same amino acid sequence, members of the CLIC family have recently been described as part of the novel metamorphic protein class.[3,4]

The restricted divergence and high level of conservation shared among CLIC proteins attests to a significant cellular function. However, despite increasing data describing their physiological function[5−9] and disease associations including cancer[10−12] and more recently intellectual disability,[13] their molecular function remains unclear.

In addition to ion channel activity, many other functional roles have been ascribed to the CLIC proteins. These include redox regulation, enzymatic, and transcription factor activity.

Several CLIC members have also been described as scaffolding proteins thought to couple the membrane to the cytoskeleton (for further detailed review, see ref 2). However, the precise role of both the soluble and integral membrane forms of CLIC1 is not fully understood. A complete understanding of the biological importance of the metamorphic transitions that occur as CLIC1 inserts into the bilayer is also hampered by a lack of structural evidence supporting a multimeric integral membrane state as would be necessary for ion channel conductance.

To date, the crystal structures of four soluble monomeric vertebrate CLICs—CLIC1 (Figure 1a),[14] CLIC2,[15] CLIC3,[16] and CLIC4[17]—and two invertebrate CLIC-like proteins—*Drosophila melanogaster Dm*CLIC and *Caenorhabditis elegans* EXC4[18]—have been determined. These soluble, monomeric CLIC proteins have all been found to adopt a conserved glutathione S-transferase (GST) family fold consisting of an N-terminal thioredoxin domain and a compact, all-helical, C-terminal domain.
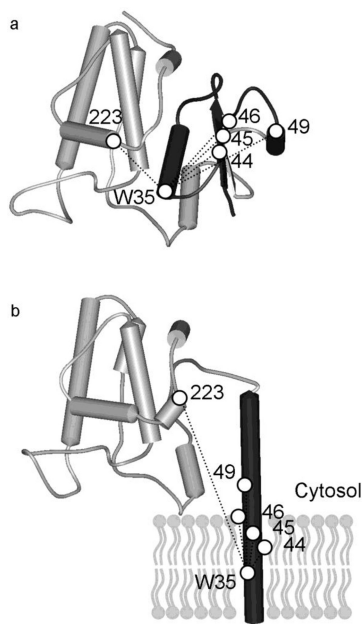
Figure 1. (a) Schematic representation of the structure of the CLIC1 reduced monomer (PBD 1K0M[20]) and (b) model of the CLIC1 integral membrane form as previously generated from FRET distance constraints.[31] Residues 24−58 (*black*) are modeled as a single transmembrane helix. In this study, FRET distances were measured in solution and upon interaction with the membrane under oxidative conditions between Trp35 and 5 IAEDANS labeled sites as mapped onto both structures: 44, 45, 46 in the transmembrane domain; 49 on the border of the transmembrane domain and native cysteine 223 within the C-domain. The approximate boundaries of the lipid bilayer are indicated.

Structural homology of the CLICs to the GST superfamily of globular cytosolic enzymes, in addition to the unusual structural characteristics of the CLIC proteins, initially led to some controversy as to whether the CLICs strictly form ion channels or act as some form of ion channel regulator. This view has been dispelled with several independent groups having now demonstrated that soluble recombinant CLIC proteins, including CLIC1, CLIC2, CLIC4, and CLIC5, can integrate into artificial bilayers in the absence of other cellular components to reproducibly form electrophysiologically characterized ion channels.[15,19−25]

In order to dock and insert into the membrane and assemble into an active ion channel, the CLIC protein must undergo a major structural rearrangement of the globular GST-like monomer fold. It is now relatively well established that the CLICs possess a single N-terminal transmembrane domain (∼Cys24 through Val46 of CLIC1) that transverses the membrane in a single pass.[26−28] Intrinsic flexibility of this N-terminal region in the globular, soluble form has been shown for CLIC1. Under oxidizing conditions, CLIC1 can form a second stable soluble structure, namely a noncovalent, all helical dimer.[20] Metamorphosis between the CLIC1 monomer and oxidized dimer form involves major structural rearrangement of the N-terminal domain with formation of an intramolecular disulfide between Cys24 and Cys59. This conformational switch results in exposure of a large hydrophobic surface within the monomer which forms the interface between the two dimer subunits. The structural and physiological relevance of the oxidized induced dimer state and its relationship to CLIC1 ion channel form remain unclear.

However, oxidative conditions have also been shown to enhance the interaction between CLIC1 and the membrane bilayer and subsequent channel activity.[20,27] One hypothesis is that the hydrophobic surface formed upon oxidation may allow CLIC1 to dock to the membrane and, in doing so, form a precursor to the CLIC1 integral membrane state.[20] Recent chemically induced unfolding and hydrogen−deuterium exchange experiments on the soluble form of CLIC1 also identify this N-terminal transmembrane region as possessing increased flexibility at low pH as would be encountered at the membrane surface.[29,30]

To date, our efforts to stabilize CLIC1 in its transmembrane configuration have been unsuccessful. However, a recent *in vitro* fluorescence resonance energy transfer (FRET) study from our group has indicated that CLIC1 does indeed undergo a large structural rearrangement in the presence of the membrane.[31] Based on these results, a model was proposed in which the N-domain folds away from the C-domain as CLIC1 inserts into the bilayer (Figure 1b).[31] In order to then form a pore through the bilayer from the single N-terminal transmembrane domain, several CLIC1 subunits must interact to form a multimeric species. The structure of the CLIC1 channel and the stoichiometry of the CLIC1 monomers that form the channel are unknown.

To fully understand the molecular function of the enigmatic CLIC1 protein, it is essential we characterize its integral membrane ion channel form. In this paper, we have extended our *in vitro* FRET approach to examine the integral membrane form of CLIC1 and obtain the first structural evidence of an oligomeric membrane state. FRET was used to monitor structural changes within the CLIC1 monomer as it converts from the soluble form to the integral membrane form by measuring the intramolecular distances between the single native tryptophan residue (Trp35), located in the trans-membrane domain, and a series of five IAEDANS-labeled cysteine residues (Figure 1a). The change in the five intramolecular FRET distances upon oxidation in a membrane environment showed good agreement with our current model of transmembrane extension. To monitor the oligomerization of CLIC1 in the membrane, intermolecular FRET was performed by mixing pools of CLIC1 modified with either donor or acceptor fluorophores. Significant intermolecular FRET was only observed upon oxidation of CLIC1 in the presence of the membrane. This FRET data was found to be consistent with a model of a large oligomeric species consisting of approximately 6−8 subunits.

■ MATERIALS AND METHODS

CLIC1 Mutant Constructs. We have previously developed a site-directed-labeling strategy for CLIC1 which preserves the functional and structural redox response of the protein.[31] This method was employed with some modification. The gene for human CLIC1 (NP_001279) was cloned into the pET28a vector (Novagen) at the NdeI and NotI cloning sites. The resulting expression construct consisted of an N-terminal 6x His-tag and thrombin cleavage site, followed by the complete CLIC1 coding sequence. The QuikChange site-directed mutagenesis kit (Stratagene) was used to mutate four of the six native CLIC1 cysteines to alanine (C89A, C178A, C191A, C223A). The remaining two native CLIC1 cysteines, Cys24 and Cys59, were not modified. Individual cysteine mutations (T44C, T45C, V46C, K49C, and native C223) were then

introduced into this mutant template as sites for fluorescent labeling.

Expression and Purification of CLIC1 Oxidized Dimer. The CLIC1 mutants were transformed into *Escherichia coli* BL21(DE3) competent cells (Stratagene) for expression. Cells were grown in 2xYT media at 37 °C prior to induction with 1 mM IPTG at mid log growth phase. The cell culture was then allowed to grow for a further 16 h at 20 °C before lysis. Soluble CLIC1 protein was isolated by binding to Ni-NTA resin (Novagen) and eluted via cleavage of the His-tag with 50 NIH units of bovine plasma thrombin per liter of cell culture for 16 h (Sigma-Aldrich). All purified CLIC1 protein consisted of the CLIC1 sequence with an extra three residues at the N-terminus (Gly-Ser-His) as a result of the thrombin cleavage site in the fusion construct.

CLIC1 Cys24 has been shown to be necessary for function.[20,21] Hence, it was necessary to retain this native cysteine residue in all mutants and ensure it remained unmodified during labeling. Upon formation of the oxidized CLIC1 dimer, Cys24 and Cys59 form a disulfide bond and are therefore protected from modification during the labeling procedure.[31] Thus, as both Cys24 and Cys59 are retained in all the CLIC1 labeling constructs, in the oxidized dimer state only the single introduced cysteine residues can be labeled. Subsequent reduction of the labeled CLIC1 then returns it to its monomeric state. The CLIC1 oxidized dimer form was obtained for each mutant by treatment with 2 mM hydrogen peroxide in phosphate buffered saline (pH 7.4) for 2 h, after which the dimer form was isolated via size exclusion chromatography, as previously described (Supporting Information, Figure S1).[31]

Fluorescent Labeling. The CLIC1 oxidized dimer constructs were labeled with either IAEDANS (5-((((2-iodoacetyl)amino)ethyl)amino)naphthalene-1-sulfonic acid) or IAF (5-iodoacetamidofluorescein) fluorescent labels. A 10-fold molar excess of label was added to ~2 mg/mL of CLIC1 dimer in assay buffer (150 mM NaCl and 50 mM Tris-HCl pH 8.0). The protein and label were allowed to react for 16 h at 4 °C before removing excess label via extensive dialysis against assay buffer. Reducing agents were excluded from the labeling reaction to maintain the Cys24-Cys59 intramolecular disulfide bond and allow for specific individual labeling of the remaining free single cysteine (44, 45, 46, 49, or 223).

To obtain labeled CLIC1 in the monomer form, the single cysteine labeled dimer constructs were treated with the reducing agent DTT. The labeled CLIC1 dimer was incubated with 10 mM DTT at 4 °C for at least 2 h. The DTT concentration was then reduced to <0.01 mM by dialysis against assay buffer. Conversion of the labeled CLIC1 dimer to monomer was assessed by size exclusion chromatography on a Superdex 75 10/300 GL (Tricon) and native gel electrophoresis, as previously described.[20]

Labeling ratios were calculated spectrophotometrically by determining the protein concentration by a BCA protein assay (Pierce) and using molar absorption coefficients of ε of 6100 M^{-1} cm^{-1} at 336 nm for IAEDANS[32] and 48 700 M^{-1} cm^{-1} at 495 nm for IAF.[33] Where possible, all steps involving IAEDANS and IAF were performed in the dark to prevent photobleaching.

Liposome Preparation. Liposomes were prepared as previously described.[27,31] Briefly, soybean phosphatidylcholine (Sigma, P-5638) and cholesterol (Sigma, C-8667) were dissolved in chloroform and mixed at a ratio of 10:1 (w/w)

before being dried under nitrogen. Following rehydration in assay buffer, liposomes were extruded at 400 nm using a LiposoFast Basic apparatus (Avestin) to produce unilamellar liposome vesicles. Liposome integrity was ensured by storing vesicles on ice and using them within 24 h of rehydration. As observed here and previously, optimal membrane binding of CLIC1 to liposome vesicles, as judged by sucrose loaded vesicle sedimentation experiments, occurred within this time frame (see Supporting Information, Figure S2).[27]

Fluorescent Resonance Energy Transfer (FRET) Analysis. Steady-state fluorescence intensity spectra were recorded at room temperature (22 °C) on a Perkin-Elmer LS50B fluorimeter operated in ratio mode with spectral bandwidths of 3–6 nm. Subtraction of liposome only spectra was used to correct for background liposome scatter. Inner filter and self-absorption effects were minimized by ensuring that the absorbance of all samples at the excitation wavelength was kept below 0.05.

For FRET to occur, energy absorbed by the donor molecule (either Trp35 or IAEDANS) is transferred to the paired acceptor (either IAEDANS or IAF, respectively) through dipole−dipole interaction. FRET results in a decrease in donor fluorescence intensity in the presence of the acceptor and corresponding increase in the acceptor intensity. The fraction, or efficiency of energy transfer E, is dependent on the distance R between the donor and acceptor labels and is determined from the decrease in donor fluorescence according to

$$E = 1 - \frac{F_{DA} - F_D(1 - f_A)}{F_D f_A} \tag{1}$$

where F_D is the fluorescent intensity of the donor in the absence of the acceptor, F_{DA} is the fluorescent intensity of the donor in the presence of the acceptor and, f_A is the fractional labeling of the acceptor site.

Intramolecular FRET between Trp35 and IAEDANS (Cys 44, 45, 46, 49, and 223). Intramolecular FRET from the donor, Trp35, to four IAEDANS acceptor labeled sites within the transmembrane region (44, 45, 46, and 49) and one at the C-terminus (223) were measured both in solution and upon oxidization in the presence of the membrane. Samples were excited at a tryptophan excitation wavelength of 290 nm, and fluorescence emission was monitored from 300 to 550 nm. Fluorescence spectra were first collected for soluble CLIC1 monomer in solution for both IAEDANS labeled CLIC1 mutant (F_{DA}) and unlabeled CLIC1 (F_D) at 6 μM. A 1:250 excess of liposomes vesicles to protein ([1.4 mM] liposome final) was then added to both the F_{DA} and F_D samples followed by the addition of 2 mM H$_2$O$_2$. Spectra were recorded at 0 h(within 2 min to allow for mixing), 4 h, 8 h, and 24 h. The fluorescent intensity values to calculate E were taken at 341 nm, the maximum fluorescence emission peak for IAEDANS, and the distance (R) separating donor and acceptor labels were calculated from the measured transfer efficiencies using the Förster equation:

$$R = (E^{-1} - 1)^{1/6} R_0 \tag{2}$$

where R_0 is the critical distance at which $E = 50\%$. The value of R_0, dependent on the donor−acceptor pair, is given by

$$R_0 = 9.78 \times 10^3 [\kappa^2 n^{-4} Q_D J(\lambda)]^{1/6} \text{ (Å)} \tag{3}$$

where κ^2 is the dipole interaction orientation factor (assumed to be 2/3), n is the refractive index of the medium (1.33), Q_D is the quantum yield of the donor in the absence of the acceptor, and $J(\lambda)$ is the overlap integral, calculated from

$$J(\lambda) = \frac{\int_0^\infty F_D(\lambda)\varepsilon_A(\lambda)\lambda^4 \, d\lambda}{\int_0^\infty F_D(\lambda) \, d\lambda} \tag{4}$$

where $F_D(\lambda)$ is the fluorescence intensity of the donor at wavelength λ and $\varepsilon_A(\lambda)$ is the molar absorbance of the acceptor at λ. The quantum yield (Q_D) and the overlap integral between the Trp35 donor emission and IAEDANS acceptor absorbance ($J(\lambda)$) for CLIC1 in solution were 0.14 and 4.2×10^{-15} M^{-1} cm^3, respectively. The R_0 obtained was 22 Å for the CLIC1 Trp35-IAEDANS FRET pair, as previously reported.[31] The overlap integral ($J(\lambda)$) of the CLIC1 IAEDANS donor emission and CLIC1 IAF acceptor absorbance was calculated by numerical integration to be 1.8×10^{-15} M^{-1} cm^3, and again, the value did not change under lipid conditions. The quantum yield of CLIC1 IAEDANS was determined to be 0.58 in FRET assay buffer at 25 °C, resulting in a R_0 for the CLIC1 IAEDANS-IAF pair of 51 Å, consistent with previous values reported.[34]

Intermolecular FRET between IAEDANS and IAF (Cys 44, 49, and 223). Intermolecular FRET distances were measured between IAEDANS donors and IAF acceptors located on the same residue (44, 49, or 223) but on different CLIC1 subunits. All samples were excited at the IAEDANS maximum of 336 nm, and fluorescent intensity values were scanned over a 400−600 nm emission range. Fluorescence intensities were measured for donor plus acceptor samples (F_{DA}) which were prepared by mixing IAEDANS-labeled CLIC1 with IAF-labeled CLIC1 to a total of 2 μM in the donor-to-acceptor ratios as described below. Emission spectra were also collected for IAEDANS-labeled donor only samples (F_D) prepared using the same concentration of donor labeled CLIC1 but to a total CLIC1 concentration of 2 μM by incorporation of unlabeled CLIC1. The efficiency of energy transfer was determined from the decrease in fluorescence intensity of IAEDANS at a wavelength of 460 nm, as emission due to IAF is relatively low but significant emission due to IAEDANS still occurs at this point.

To seek evidence of intermolecular FRET and thus oligomerization, FRET was first measured for a 1:1 molar ratio of IAEDANS-labeled to IAF-labeled CLIC1 individually at each of the three targeted sites (44, 49, and 223). Emission spectra were recorded at 0 h (within 2 min to allow for mixing), 4 h, and 24 h after mixing for a series of four different conditions: (i) CLIC1 monomer in solution without oxidation, (ii) CLIC1 monomer in solution under oxidizing conditions (addition of 2 mM H_2O_2), (iii) CLIC1 monomer upon addition of a liposome vesicles without oxidation (1:250 protein to liposome ratio), and (iv) CLIC1 monomer upon addition of liposome vesicles (as for condition iii) followed by oxidizing conditions (as for condition ii).

To allow for modeling of the CLIC1 oligomer form, the donor to acceptor ratio was varied using two approaches. In method A, the fraction of IAEDANS donor labeled CLIC1 (f_D) was varied by incorporating unlabeled CLIC1 (f_U) in place of donor labeled CLIC1. The fraction of IAF acceptor labeled CLIC1 (f_A) was kept constant at 0.50. Hence, $f_D + f_A + f_U = 1$. Using this method, the efficiency of energy transfer was

determined for CLIC1 labeled at residues 44, 49, and 223 upon the addition of liposomes followed by addition of H_2O_2 to 2 mM (condition iv from above) at a 4 h time point. FRET was measured at four different f_D values (0.50, 0.25, 0.10, and 0.05).

To model the geometric conformation of the CLIC oligomer state, in method B, the value of f_D was varied from 0 to 1.0 by adjusting the relative concentration of both the donor and acceptor labeled CLIC1 protein without the incorporation of unlabeled protein. Hence, $f_D + f_A = 1$. Method B was performed for 12 labeled samples at varying f_D values for CLIC1 labeled at residue 223. Again, FRET was collected upon the addition of liposomes followed by addition of H_2O_2 to 2 mM (condition iv from above) at a 4 h time point.

Modeling of the CLIC1 Oligomeric Species. "Exi-FRET", a software package developed by Corry et al. (2005), can be used to model FRET arising from complex geometrical systems containing multiple donors and acceptors that cannot be described by a single distance model. An application of the ExiFRET program to model conformational changes associated with the gating of the MscL mechanosensitive channel was previously demonstrated, and thus the program is also well suited for our purposes.[35] The program utilizes a Monte Carlo scheme to relate the efficiency of energy transfer to a distribution of single protein label sites (either unlabeled or labeled with donor or acceptor) where each site is placed in an oligomer with n-fold symmetry. Each model is specified by two parameters: n the order of the rotational symmetry and r the radius of the label site from the symmetry axis.[36] We used ExiFRET to calculate the FRET efficiency expected to arise for a series of oligomeric CLIC1 species varying in both the number of subunits (n), where n was varied from 2 to 12 (noting that each subunit contains one label site), and the radius (r) where r was varied from 0 to 140 Å in 2 Å steps. The program provides an E value for a multimeric species as a function of n and r, to which the observed FRET efficiency was then related. The ExiFRET "P Donor" input corresponds to the fraction of donor labeled protein (f_D), while the "labeling efficiency" corresponds to the remaining fraction of protein that is acceptor labeled ($f_A/(1 - f_D)$). For the IAEDANS-IAF donor−acceptor pair, the R_0 value of 51 Å was used, as determined from eqs 3 and 4. The calculation for E assumes a random mix of either unlabeled or donor or acceptor labeled sites distributed in a symmetrical ring confined to two dimensions. That is, the assumption was made that any CLIC1 oligomeric species forms a rotationally symmetric complex within the plane of the lipid bilayer. No attempt was made to model higher order assemblies of rotationally symmetric pore complexes, as would be expected from the electrophysiological characterization of the CLIC1 channel.[25] Nonspecific FRET between oligomeric species was most likely avoided due to the low protein concentration (2 μM) used.

Comparison of the modeled E values calculated by ExiFRET to the experimental FRET data obtained upon oxidation of CLIC1 in the presence of the membrane at 4 h was used to determine the best fit parameters, n and r, for the CLIC1 oligomeric species. For method A, where experimental E values were obtained by the incorporation of unlabeled CLIC1 in the FRET sample, the ExiFRET E values for comparison were generated for a range of radii from 0 to 140 Å for four oligomeric models ($n = 2, 4, 8,$ and 12). For method B, where both f_D and f_A were varied, FRET obtained E values were compared to ExiFRET generated E values for f_D ranging from 0 to 1.00. Using the ExiFRET calculated E values, curves of f_D

Table 1. Intramolecular FRET Efficiency (E) and Distances (R) Calculated from Trp35 to IAEDANS Labeled Residues in the Soluble and Membrane CLIC1 States[a]

IAEDANS acceptor site	labeling efficiency (%)	FRET					crystal structure/modeled distances	
		E_{sol}	R_{sol} (Å)	E_{+lip}	E_{mem}[b]	R_{mem} (Å)	$R_{monomer}$[c] (Å)	R_{model}[d] (Å)
44	93 ± 11	0.42 ± 0.06	23.2 ± 0.9	0.35 ± 0.05	0.32 ± 0.07	24.9 ± 1.3	14.4	14.8
45	80 ± 12	0.38 ± 0.06	23.9 ± 1.0	0.37 ± 0.06	0.37 ± 0.08	24.1 ± 1.4	16.6	15.9
46	82 ± 11	0.24 ± 0.04	26.5 ± 0.9	0.32 ± 0.05	0.35 ± 0.06	24.5 ± 1.0	19.8	17.1
49	89 ± 12	0.13 ± 0.02	30.3 ± 0.8	0.28 ± 0.04	0.34 ± 0.05	24.5 ± 0.8	28.0	21.6
223	101 ± 12	0.58 ± 0.07	20.9 ± 1.1	0.19 ± 0.03	0.02 ± 0.08	40.8 ± 12.5	13.1	41.0

[a]Corresponding distances derived from the CLIC1 monomer crystal structure and CLIC1 integral membrane model are presented for comparison. [b]Calculated as E_{+lip} arises from a mixed population of two conformers: 35% soluble (E_{sol}) and 65% membrane associated CLIC1 (E_{mem}), respectively. [c]Distance between Trp35 Cα and Cα at label site obtained from CLIC1 monomer crystal structure (Protein Data Bank entry 1K0M, Figure 1a). [d]Distance between Trp35 Cα and Cα at label site using our CLIC1 monomer integral membrane model, as shown in Figure 1b.[31]
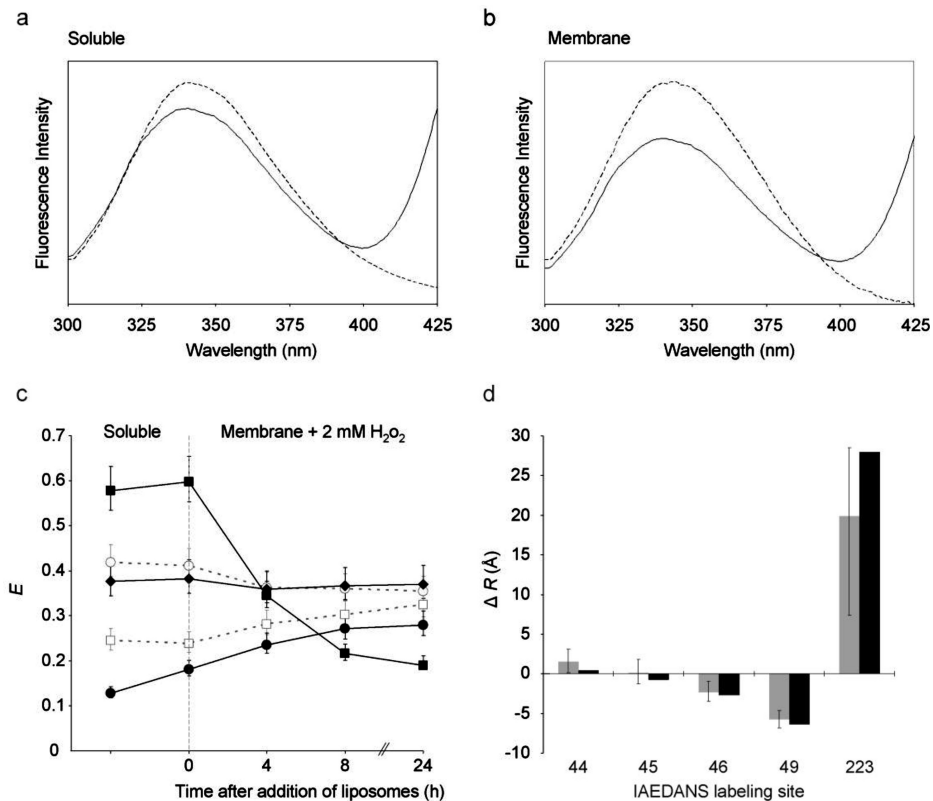

Figure 2. Intramolecular FRET between the single native Trp35 and IAEDANS labeled cysteines at residues 44, 45, 46, 49, and 223. (a) Representative fluorescence spectra of energy transfer from Trp35 to IAEDANS-49 in the soluble state and (b) following oxidation in the presence of the membrane state at 24 h. Donor only, dashed line; donor–acceptor, solid line. (c) Efficiency of energy transfer (E) from Trp35 to IAEDANS labeled residues in the soluble state and 24 h time course following the addition of lipid and 2 mM H_2O_2 (44, open circle; 45, closed diamond; 46, open square; 49, closed circle; 223, closed square). (d) Change in FRET distance (ΔR) from Trp35 to each of five IAEDANS labeled residues observed between the soluble and membrane states at 24 h (gray). Change in distance expected for corresponding residues sites calculated from the CLIC1 monomer crystal structure and integral membrane model as shown in Figure 1 (black).

versus E for a given n (for values from 2 to 12, inclusive) and r (0 to 100 Å) were generated at 2 Å radius intervals. The set of experimentally determined E values was then matched to the model of best fit using a nonlinear regression analysis in Mathematica by varying the two parameters n and r.

■ RESULTS

Fluorescent Labeling of CLIC1. Our strategy to achieve site-specific cysteine labeling of CLIC1 ensures that Cys24, a functionally important cysteine residue, is protected from modification by the extrinsic fluorescent label.[31] High efficiency

of labeling (~100%) was achieved for the five engineered single cysteine residues (44, 45, 46, 49, and native Cys223) in the oxidized dimer form (see Supporting Information, Figure S3). The labeled monomeric CLIC1 state for all five labeled constructs was successfully obtained for FRET analysis following the reduction of the Cys24-Cys59 disulfide (see Supporting Information, Figure S4).

Intramolecular FRET: Transmembrane Extension. Intramolecular FRET was detected between the Trp35 donor residue and five IAEDANS-modified cysteine residues, four located within the N-domain (44, 45, 46, and 49) and one in the C-domain (223). The three consecutive N-domain residues

(44, 45, and 46) were targeted as the expected change in distances from Trp35 to each upon lipid addition were most advantageous to confirm the extension of the CLIC1 transmembrane region, as suggested by the model (Table 1). The residue 49 was also chosen as the expected distance change was greatest from Trp35 to this residue (decrease of 6.5 Å), easily detectable by the FRET technique. The efficiency of energy transfer between each donor−acceptor pair was measured by the relative decrease in the tryptophan donor emission peak (341 nm). Representative spectra of the intramolecular FRET observed from Trp35 to IAEDANS label at residue 44, both in solution and following the addition of liposomes, are shown in parts a and b of Figure 2, respectively. For all five probe pairs, FRET was observed with CLIC1 both in solution and upon the addition of liposomes. In the presence of liposomes, the greatest change in FRET efficiency was seen upon the addition of H_2O_2 up to a 24 h time point (Figure 2c). Lipid integrity prevented measurement of time points beyond 24 h. There was no significant change in the FRET efficiency measured in the presence of the liposomes without oxidation (data not shown).

As shown in Figure 2c, upon the addition of the liposomes and oxidizing conditions, the value of E was observed to notable decrease over time for two out of the five label pairs: Trp35 to Cys44 and, most dramatically, for Trp35 to Cys223. The value of E was measured to increase with time for two further FRET pairs, Trp35 to Cys46 and Trp35 to Cys49, while the fifth FRET pair, Trp35 to Cys45, did not show any significant change in E. For all five FRET pairs, the E values determined were observed to plateau between 4 and 24 h such that the maximal change between E values obtained in the soluble state (E_{sol}) and in the presence of the membrane were taken at the 24 h time point (E_{+lip}, Table 1).

The Förster equation was used to calculate the corresponding FRET distances in the CLIC1 soluble monomeric state (R_{sol}) and the CLIC1 membrane associated form (R_{mem}) (Table 1). The value of E_{mem}, or the efficiency of energy transfer arising from the membrane associated portion of CLIC1 protein at 24 h, was calculated from both E_{sol} and E_{+lip} on the basis that 35% of the measured E value under oxidative conditions results from noninserting CLIC1 that remains in the soluble monomer form (see Supporting Information, Figure S2).[27] FRET distances for R_{mem} were subsequently obtained from E_{mem}.

Comparison of Intramolecular FRET Distances with the CLIC1 Crystal Structure and the Transmembrane State Model. Calculations of FRET distances expected for the CLIC1 monomeric soluble state obtained from the crystal structure distance (PDB 1K0M) between the Cα of Trp35 and Cα of the IAEDANS labeled residue ($R_{monomer}$, Table 1 and Figure 1a) were all in good agreement with the corresponding measured R_{sol} FRET distances. The small ~2−9 Å deviation of the experimental FRET distances compared to the crystal structure distances are not unexpected when probe length, flexibility, and orientation are considered.[37] Comparison of the FRET distances obtained in the membrane state (R_{mem}) to our model of the CLIC1 integral membrane form, previously generated from FRET distance constraints (R_{model}, Table 1 and Figure 1b), also showed good agreement.[31] Again, the FRET distances measured for the membrane state were all only slightly longer (~6−10 Å) than those expected from our model.

Intermolecular FRET: Detection of CLIC1 Oligomerization. Intermolecular FRET was measured between IAEDANS donor and IAF acceptor labels located at the same residue, but on different CLIC1 molecules. FRET is only observed when the dipole−dipole interaction between the donor and acceptor labels falls within the upper limit of detection for the probe pair, ~100 Å for IAEDANS-IAF, thereby indicating the formation of a multimeric CLIC1 species. FRET was initially performed in the simple case of a 1:1 mix of donor and acceptor labeled CLIC1 at residue 44, 49, or 223. FRET was measured both in solution and in the presence of liposomes, with and without the addition of the oxidizing agent. Representative FRET spectra for CLIC1 labeled at residue 223 collected under these four experimental conditions (i−iv) are shown in Figure 3. Only
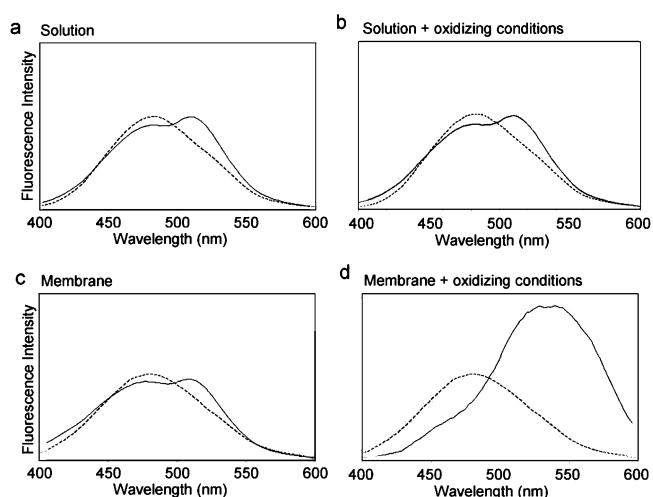

Figure 3. Intermolecular FRET between IAEDANS (donor) and IAF(acceptor) labels located at Cys223 of CLIC1. (a) CLIC1 reduced monomer in solution: condition i; (b) following oxidation with 2 mM H_2O_2: condition ii; (c) CLIC1 reduced monomer in the presence of liposomes without additional redox conditions: condition iii; and (d) following oxidation with 2 mM H_2O_2: condition iv. All spectra were recorded at an excitation wavelength of 336 nm at 4 h for a 1:1 ratio of donor to acceptor labeled CLIC1. Donor only, dashed line; donor−acceptor, solid line.

upon the oxidation of CLIC1 in the presence of the liposomes (condition iv) over time was considerable intermolecular energy transfer, and thus evidence of oligomerization, observed. A dramatic decrease in the emission peak of the donor was accompanied by an increase in the emission of the acceptor, corresponding to energy transfer (Figure 3d). The maximal value for the efficiency of energy transfer for all three labeling sites were observed at the 4 h time point with values for E ranging from 0.40 to 0.49 (Table 2 and Supporting Information, Table S1).

In solution, little FRET ($E_{solution} \leq 0.09$) was observed for all three labeled residues (Table 2; see Supporting Information Table S1 for data obtained at 0 and 24 h). No notable increase in FRET was observed upon the addition of the oxidizing agent ($E_{solution}$ + 2 mM H_2O_2), with values again ≤0.09 (Table 2). Upon the addition of liposome vesicles, again, no significant FRET (≤0.09) was seen over time ($E_{membrane}$). It is expected that a proportion of the monomeric CLIC1 will form oxidized dimer in solution. Therefore, the proportion of dimer formed in the absence of a reducing agent (i−iii) can be calculated from the E values. The amount of dimer that was found to occur

Table 2. Intermolecular FRET Efficiency (E) Measured between IAEDANS and IAF Labeled CLIC1[a]

labeling site	$E_{solution}$	$E_{solution} +$ 2 mM H_2O_2	$E_{membrane}$	$E_{membrane} +$ 2 mM H_2O_2
44	0.03 ± 0.01	0.03 ± 0.01	0.03 ± 0.01	0.40 ± 0.06
49	0.09 ± 0.02	0.04 ± 0.02	0.06 ± 0.02	0.46 ± 0.06
223	0.06 ± 0.02	0.09 ± 0.02	0.04 ± 0.02	0.49 ± 0.07

[a]All E values were obtained using a 1:1 mix of donor to acceptor labeled protein with the labels located at the same residue but on different CLIC1 molecules. FRET was measured in solution and in the presence of the membrane, both in the absence of additional redox conditions and following oxidation at a 4 h time point.

upon oxidation in solution for the three label sites, assuming the predicted probability of formation of a dimer donor–acceptor pair had occurred, was 9 ± 7% for 44, 13 ± 9% for 49, and 22 ± 9% for 223. This calculated amount of dimer formed upon reoxidation of our labeled monomeric CLIC1 is low but consistent with the yields obtained upon initial purification of the oxidized dimer (Supporting Information, Figure S1).

Intermolecular FRET: Modeling the CLIC1 Oligomer Form. The relationship between the efficiency of energy transfer between a donor and acceptor label pair separated by a single distance is well established. However, in the case of our intermolecular FRET, the situation is more complex as the CLIC1 subunits may assemble into an oligomeric protein form and therefore contain a random mix of unlabeled CLIC1 plus CLIC1 labeled with IAEDANS donor and IAF acceptor labels. Hence, the efficiency of energy transfer observed under oxidative conditions in the presence of liposomes (Figure 3d) is related not only to the distance separating the donor and acceptor labels but also to the fraction of donor and acceptor labeling and the number (n) of interacting subunits in the oligomeric state.

Two different strategies were used to vary the degree of labeling in the CLIC1 oligomeric integral membrane form. In the first (method A), the fraction of acceptor labeled protein was held fixed at $f_A = 0.5$, while the fraction of labeled donor (f_D) protein was varied by the addition of unlabeled CLIC1 (f_U). For each experimental condition, the measured E values were plotted on the curves of ExiFRET calculated E values as a function of label radius for models with 2-, 4-, 8-, and 12-fold symmetry, representing dimers, tetramers, octamers, and dodecamers, respectively (Figure 4). When the fraction of donor label $f_D \leq 0.25$, the experimental E values for the three label sites (44, 49, and 223) are all greater than the calculated values of the dimer model, precluding this as the integral membrane form of CLIC1. The best correlation between the experimental FRET data and the modeled curves can be seen for the two larger oligomeric species of $n = 8$ and $n = 12$. The octamer model reveals the narrowest range of corresponding radii of ~48−59 Å for labeled residue 44, ~55−64 Å for 49, and ~58−68 Å for 223.

Using a second strategy (method B), the fraction of donor and acceptor labeled protein was varied between 0 and 1.0 without the addition of unlabeled CLIC1. These data were only collected for labels at residue Cys223 in CLIC1. Experimentally measured E values were compared to ExiFRET predicted E values over the f_D range of 0−1.0. Model data with radii ranging from 1 to 100 Å at 2 Å intervals were generated for each oligomeric species from $n = 2$ to 12, inclusive. The experimental FRET data were fitted to the ExiFRET generated model data using nonlinear regression analysis (Figure 5). The
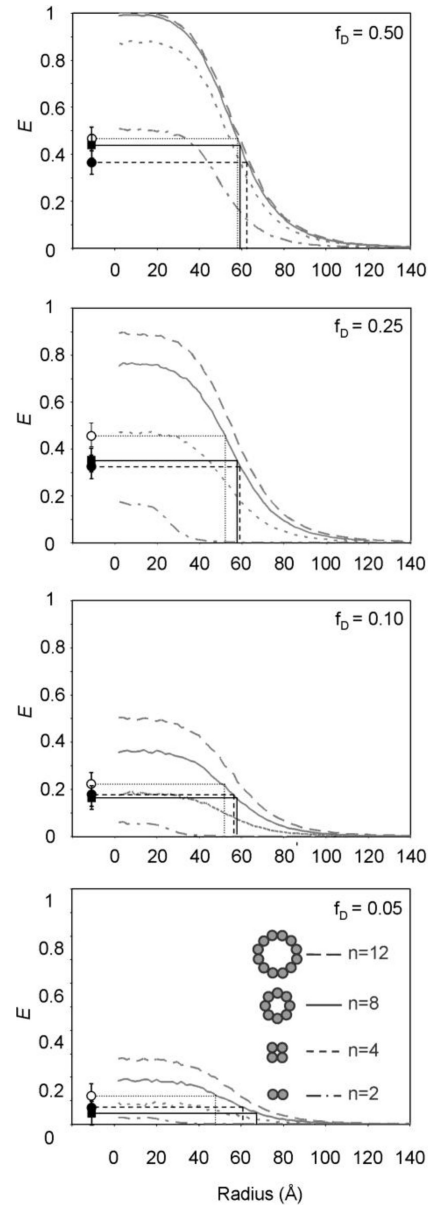

Figure 4. Intermolecular FRET measured between IAF and IAEDANS at residue 44, 49, or 223 following oxidation in the presence of the membrane. f_D was varied by incorporation of unlabeled CLIC1, while f_A was kept constant at 0.50 (method A). Corresponding ExiFRET curves of predicted E values for specfied radius for models of a dimer ($n = 2$), tetramer ($n = 4$), octomer ($n = 8$), and dodecamer ($n = 12$) are shown. The fit of FRET efficiency values and extrapolated radial distance measured for residues 44 (open circle), 49 (closed circle), and 223 (closed square) to the octamer curve are shown.

best fit parameters from the regression were with an n value of 7 ± 1 with a 95% confidence interval of $n = 5−9$ and an r value of 66 ± 3 Å with a 95% confidence interval of $r = 59−73$ Å. By its nature, the regression analysis does not account for any possible systematic errors. In Figure 5a, it can be seen that the regression fit (denoted by the 0.95 error ellipse) correlates well with the minimum mean-square error estimator (represented by the contours). The corresponding curve of best fit to the experimental data from the nonlinear regression analysis is shown in Figure 5b, and a schematic representation of such a large oligomeric configuration and corresponding radial distance for residue 223 is provided in Figure 5c.
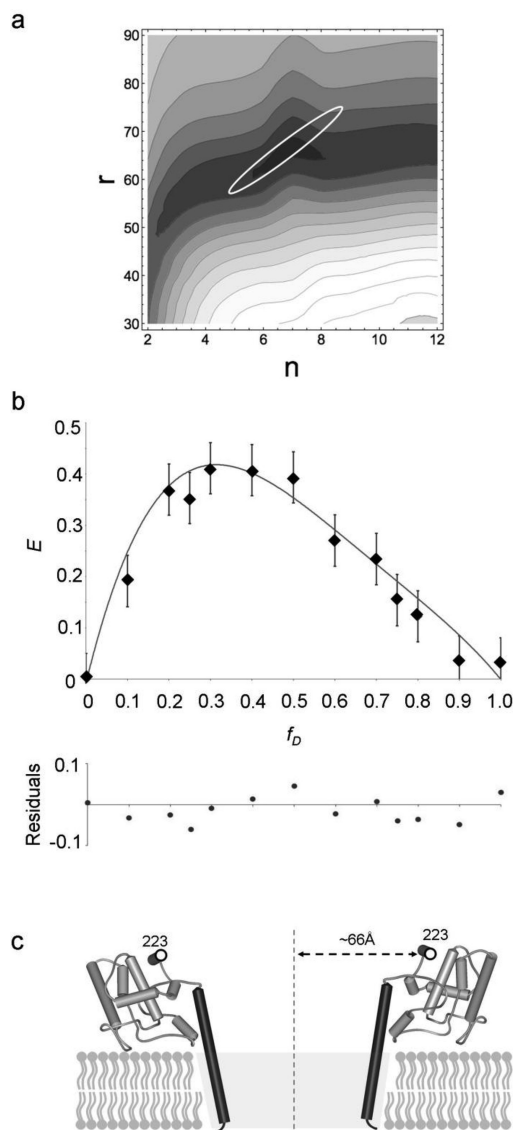
Figure 5. Modeling of intermolecular FRET measured between IAEDANS and IAF at residue 223 following oxidation in the presence of the membrane. FRET f_D values were measured by adjusting the ratio of donor to acceptor labeled CLIC1 (method B). (a) The experimentally determined E values were modeled by nonlinear regression against ExiFRET generated E values where the number of subunits (n) and the radius (r) were varied. The contours represent the RMSE value of the model to the experimental data. The contours are evenly spaced at increments of 0.04 with the lowest contour being 0.04 (black) and the highest being 0.52 (white). The error ellipse represents the region of best fit by the nonlinear regression analysis at the 95% confidence level ($n = 5–9$, $r = 59–73$) and correlates with the contour of lowest RMSE value (<0.04). The best fit parameters from the regression reveal $n = 7 \pm 1$ and $r = 66 \pm 3$ (R^2 value of 0.985). (b) The corresponding curve of best fit ($n = 7$, $r = 66$) obtained from nonlinear regression analysis shown in (a). The residual E values for corresponding solution exhibit a random pattern. (c) Schematic representation of CLIC1 oligomeric configuration indicating the radius of 66 Å.

■ DISCUSSION

Although it was shown over 10 years ago that the soluble monomeric globular form of CLIC1 could self-integrate into lipid bilayers to form an ion channel,[14,24] there has been little progress into unveiling the structure of the integral membrane

form. A recent *in vitro* FRET study from our group provided the first direct evidence of CLIC1 structural rearrangement upon interaction with the membrane and proposed a model where there was a large-scale unfolding of the N-terminal transmembrane domain away from the C-domain as it inserts into the bilayer.[31] Here we use FRET measurements to show that there is indeed a large-scale structural rearrangement in CLIC1 upon membrane insertion. We also provide the first experimental evidence that the integral membrane form of CLIC1 comprises a large oligomer, where a CLIC1 oligomer of 6–8 subunits best fits the intermolecular FRET data for the integral membrane form.

To date, there is no high-resolution structure for the integral membrane form of CLIC1. Our previous FRET and EPR studies produced the first model for the integral membrane form of CLIC1 based on FRET distances between labels on three native cysteines (Cys89, Cys178, and Cys223) and native Trp35.[31] The model was developed using a rigid body simulation constrained by the experimentally determined FRET distances. However, the model assumed that residues Cys24 to Val46 formed a transmembrane helix, as was previously proposed.[20,22,29]

In the present study, we have used FRET to measure distances between the single native Trp35 to a series of introduced labeled cysteines around the C-terminal boundary of the transmembrane region (44, 45, 46, and 49) and to native Cys223. These four new FRET measurements are consistent with the transmembrane region of CLIC1 (Cys24 to Val46) adopting a helical conformation in the membrane. This is the first experimental data that is consistent with the helical model for the CLIC1 transmembrane domain. The insertion of the N-terminal transmembrane domain into the bilayer as an extended helix is thus assumed to form the integral part of the conductance pore at the symmetry axis of the resulting oligomeric species.

The intermolecular FRET measurements presented here are also the first direct evidence that CLIC1 forms an oligomer in the integral membrane form. Assuming that this oligomeric form comprises a structure with rotational symmetry, the FRET data are best fit by oligomeric model where $n = 7 \pm 1$ and $r = 66 \pm 3$ Å. Reasonable fits are also evident in the range of $n = 5–9$ with corresponding radius range of 59–73 Å (Figure 5). This is the first structural estimate of the oligomeric state of the CLIC1 channel form.

The FRET measurements for the intramolecular structural change between the soluble CLIC1 monomer and the integral membrane form and also the intermolecular FRET measurements for revealing the presence of a membrane induced oligomeric species, as carried out in the present work, are superior to those presented in our previous work.[31] The key difference is that the starting species in this study is the reduced CLIC1 monomer, presumably the native, cytoplasmic species, as opposed to the oxidized CLIC1 dimer used in the previous work. Although the CLIC1 oxidized dimer form added to membranes is known to form active ion channels similar to those observed *in vivo*,[20] fluorescence quenching and sucrose-loaded-vesicle membrane binding studies suggest that a greater proportion of membrane associated CLIC1 is obtained upon oxidation of CLIC1 monomer in the presence of the membrane (~60–70% as opposed to ~30% for dimer) (Supporting Information, Figure S2).[27] Hence, the advantages of measuring the change in FRET between the soluble CLIC1 initially in the monomer form and upon the addition of membrane are 2-fold;

only a single distance is present in the soluble state and the population of membrane associated CLIC1 is higher.

As a control for the FRET technique, a good agreement was found between the FRET distances measured in the soluble, monomeric state and those estimated from the CLIC1 crystal monomer structure for all five labeled sites (PDB 1K0M). However, the FRET technique is far more powerful when measuring a relative change in efficiency of energy transfer than when used to measure an absolute distance. Considering the uncertainties in the FRET technique, there was good correlation observed for both the difference in size and magnitude of the change in FRET distances measured between the soluble and membrane bound CLIC1 states (ΔR) to those expected from the monomer crystal structure and our transmembrane model (Figure 2d). The ΔR for the three distances measured from Trp35 to residues 44, 45, and 46 upon interaction with the membrane agreed within <2 Å of the predicted change expected for these N-domain sites. For the Trp 35 to residue 49 FRET pair, a 5.8 Å decrease in the distance upon membrane interaction was measured, which showed close agreement with the negative 6.4 Å predicted value. A larger increase of 27.9 Å was predicted for the Trp35 to 233 distance as the N-domain separates from the C-domain upon insertion into the membrane as in our model. Although an increase in distance of only 19.9 Å was experimentally measured for this probe pair, this increase in distance is still in very good agreement with the model when considering the measured E value at this such long distance is at the limit of sensitivity for the Trp−IAEDANS probe pair. Hence, a greater error in R is reflected for this longer distance pair.

Electrophysiological studies *in vitro* and *in vivo* show that the CLIC1 ion channel exhibits multiple conductance states.[25] When recombinant CLIC1 is added to an artificial bilayer, an initial small-conductance (7 ps) slow-kinetics channel or protopore is observed. With time, this evolves into a cooperatively gated high-conductance (30 ps) fast-kinetics channel that appears to couple four protopores into a mature channel.[25] The simplest interpretation of this data is that a well-defined multimer of CLIC1 (n) spans the bilayer and establishes the protopore before further tetramerising ($4n$) to form a mature channel. The protopore must comprise multiple CLIC1 subunits (probably $n \geq 4$) as the CLIC1 trans-membrane domain is short and forms a helix which can only traverse the bilayer in a single pass. It is possible that the FRET data obtained in this study may be representative of an alternate oligomeric configuration beyond the simple case of an n-symmetrical ring-like structure, as modeled here. However, upon deviation from n-symmetry around a single point, the appearance of relatively shorter FRET distances would be expected to occur, thereby biasing the efficiency of energy transfer toward significantly shorter distances. This was not observed, although we still cannot rule out other possible configurations. The simplest interpretation of the intermolecular FRET data from our modeling is that the likely 6−8 n-mer is the protopore state, in which case the mature channel would consist of 4 times as many subunits (a tetramer of 6−8 n-mer). The slight decrease observed in the intermolecular FRET at the 24 h time point (Table S1) may be evidence of the assembly of protopores to form the mature tetrameric channel over time, and this is the subject of future investigation.

Helices within membrane proteins are generally tightly packed to allow interaction over the entire width of the bilayer and enable formation of an enclosed aqueous pore. While the 66 $\pm$ 3 Å radius for a large oligomeric species of 7 $\pm$ 1 subunits, as modeled from the FRET interaction for labels located at the C-terminal residue (Cys223), is within the magnitude expected for a large multimeric protein, the radius measured for residues predicted to be within the transmembrane helix (at residues 44 and 49) in the range of 48−64 Å (Figure 4) can still be viewed to be somewhat larger than expected for a selective ion channel pore size. Some of this discrepancy may be accounted for by factoring in the additional distance contribution from the flexibility of the large fluorescent labels used. For example, the radius of the MscL mechanosensitive channel pentamer in the open state, estimated from the crystal structure to have a radius of ~30 Å, was measured as 54 Å using a similar FRET analysis as presented here.[35] Although poor selectivity of some of the CLIC family proteins may be due to a wide pore lacking specific ion-binding sites,[22] the maximum Cl− conductance observed for the CLIC1 in potassium chloride (120 pS[38]) is inconsistent with a wide water-filled pore as found, for example, in bacterial porins.

The question then becomes, how can a large CLIC1 transmembrane structure form a stable entity in the bilayer so as to be selective for chloride ions? One possibility is that the six to eight transmembrane helices form a scaffold which supports a selectivity filter structure that limits the passage of molecules through the pore. Such an arrangement would be similar to the tetrameric potassium and sodium ion channels where the transmembrane helices support the short pore helices and selectivity filter structure.[39,40] Additionally, there has been some suggestion that the conductivity of the CLIC proteins involves both the passage of anions and countercations across the pore in a similar manner to the neuronal "background" Cl− channels.[22,38] The presence of large, relatively impermeant, cations within the pore do not prevent all ion permeation but make the channel more anion-selective. A wide pore, as could naively be suggested by our CLIC1 oligomer model of between 6 and 8 subunits, would be required to accommodate such large countercations. Only through full structural elucidation of the transmembrane pore region can the true nature and mechanism of the CLIC1 pore be revealed.

Future cysteine scanning through the transmembrane regions of CLIC1 using our intermolecular FRET approach could better reveal the CLIC1 transmembrane architecture and the geometry of the pore. However, much emphasis has been placed on the potential role of the conserved Cys24 residue in defining CLIC ion channel selectivity.[21] It is unlikely that the introduction of cysteine residues within close proximity to Cys24 (or indeed Cys59) would be tolerated by our labeling strategy, as there is a high likelihood of formation of a non-native disulfide interaction which would perturb function.

While it is clear that oxidation is an important factor in CLIC1 membrane insertion, and from the results of this study, membrane induced oligomerization, the physiological trigger for CLIC1 membrane insertion is still uncertain. The exact molecular mechanism leading to formation of the CLIC1 ion channel is not known, particularly in regards as to whether membrane insertion and oligomerization are discrete or interdependent processes. There are examples in the literature of ion channels, such as the aquaporins[41] and glycerol-conducting channels,[42] that do form large helical bundles that then further oligomerize to form mature channels with multiple pores. However, the oligomeric model for the CLIC1 integral-membrane form presented herein represents a novel ion

channel architecture with each subunit contributing a single transmembrane entity to the pore in contrast to multiple transmembrane regions from a single subunit. The dynamic and metamorphic nature of the CLIC proteins continues to make them difficult although highly intriguing targets to study. Only from a high-resolution structure of the ion channel oligomer can we begin to better understand how CLIC1 functions as an ion channel.

■ ASSOCIATED CONTENT

Ⓢ Supporting Information

Experimental details of protein purification of CLIC1 mutant constructs by size exclusion chromatography (Figure S1), the sucrose-loaded vesicle sedimentation assay for measuring interaction of CLIC1 with liposome vesicles (Figure S2), UV−vis profile of the labeling of oxidized CLIC1 dimer by IAEDANS and IAF (Figure S3), and the reduction of the labeled oxidized dimer to monomeric CLIC1 (Figure S4); additional intermolecular FRET measurements performed at 0 and 24 h (Table S1). This material is available free of charge via the Internet at http://pubs.acs.org.

■ AUTHOR INFORMATION

Corresponding Author

*Tel: 61 2 9850 8294. Fax: 61 2 9850 8313. E-mail: Louise. Brown@mq.edu.au.

■ ABBREVIATIONS

CLIC, chloride intracellular channel; FRET, fluorescence resonance energy transfer; IAEDANS, 5-((((2-iodoacetyl)-amino)ethyl)amino)naphthalene-1-sulfonic acid; IAF, 5-iodoa-cetamidofluorescein; RMSE, root-mean-square error.

■ REFERENCES

(1) von Heijne, G. (2006) Membrane-protein topology. *Nat. Rev. Mol. Cell Biol. 7*, 909−918.

(2) Littler, D. R., Harrop, S. J., Goodchild, S. C., Phang, J. M., Mynott, A. V., Jiang, L., Valenzuela, S. M., Mazzanti, M., Brown, L. J., Breit, S. N., and Curmi, P. M. (2010) The enigma of the CLIC proteins: Ion channels, redox proteins, enzymes, scaffolding proteins? *FEBS Lett. 584*, 2093−2101.

(3) Murzin, A. G. (2008) Biochemistry. Metamorphic proteins. *Science 320*, 1725−1726.

(4) Goodchild, S. C., Curmi, P. M., and Brown, L. J. (2011) Structural gymnastics of multifunctional metamorphic proteins. *Biophys. Rev. 3*, 143−153.

(5) Berry, K. L., Bulow, H. E., Hall, D. H., and Hobert, O. (2003) A C. elegans CLIC-like protein required for intracellular tube formation and maintenance. *Science 302*, 2134−2137.

(6) Suh, K. S., Mutoh, M., Mutoh, T., Li, L., Ryscavage, A., Crutchley, J. M., Dumont, R. A., Cheng, C., and Yuspa, S. H. (2007) CLIC4 mediates and is required for Ca²⁺-induced keratinocyte differentiation. *J. Cell Sci. 120*, 2631−2640.

(7) Money, T. T., King, R. G., Wong, M. H., Stevenson, J. L., Kalionis, B., Erwich, J. J., Huisman, M. A., Timmer, A., Hiden, U., Desoye, G., and Gude, N. M. (2007) Expression and cellular localisation of chloride intracellular channel 3 in human placenta and fetal membranes. *Placenta 28*, 429−436.

(8) He, G., Ma, Y., Chou, S. Y., Li, H., Yang, C., Chuang, J. Z., Sung, C. H., and Ding, A. (2011) Role of CLIC4 in the host innate responses to bacterial lipopolysaccharide. *Eur. J. Immunol. 41*, 1221−1230.

(9) Ulmasov, B., Bruno, J., Gordon, N., Hartnett, M. E., and Edwards, J. C. (2009) Chloride intracellular channel protein-4 functions in angiogenesis by supporting acidification of vacuoles along the intracellular tubulogenic pathway. *Am. J. Pathol. 174*, 1084−1096.

(10) Fernandez-Salas, E., Suh, K. S., Speransky, V. V., Bowers, W. L., Levy, J. M., Adams, T., Pathak, K. R., Edwards, L. E., Hayes, D. D., Cheng, C., Steven, A. C., Weinberg, W. C., and Yuspa, S. H. (2002) mtCLIC/CLIC4, an organellular chloride channel protein, is increased by DNA damage and participates in the apoptotic response to p53. *Mol. Cell. Biol. 22*, 3610−3620.

(11) Hill, J. J., Tremblay, T. L., Pen, A., Li, J., Robotham, A. C., Lenferink, A. E., Wang, E., O'Connor-McCourt, M., and Kelly, J. F. (2011) Identification of vascular breast tumor markers by laser capture microdissection and label-free LC-MS. *J. Proteome Res. 10*, 2479−2493.

(12) Suh, K. S., and Yuspa, S. H. (2005) Intracellular chloride channels: critical mediators of cell viability and potential targets for cancer therapy. *Curr. Pharm. Des. 11*, 2753−2764.

(13) Witham, S., Takano, K., Schwartz, C., and Alexov, E. (2011) A missense mutation in CLIC2 associated with intellectual disability is predicted by in silico modeling to affect protein stability and dynamics. *Proteins 1002*, 23065.

(14) Harrop, S. J., DeMaere, M. Z., Fairlie, W. D., Reztsova, T., Valenzuela, S. M., Mazzanti, M., Tonini, R., Qiu, M. R., Jankova, L., Warton, K., Bauskin, A. R., Wu, W. M., Pankhurst, S., Campbell, T. J., Breit, S. N., and Curmi, P. M. (2001) Crystal structure of a soluble form of the intracellular chloride ion channel CLIC1 (NCC27) at 1.4-A resolution. *J. Biol. Chem. 276*, 44993−45000.

(15) Cromer, B. A., Gorman, M. A., Hansen, G., Adams, J. J., Coggan, M., Littler, D. R., Brown, L. J., Mazzanti, M., Breit, S. N., Curmi, P. M., Dulhunty, A. F., Board, P. G., and Parker, M. W. (2007) Structure of the Janus protein human CLIC2. *J. Mol. Biol. 374*, 719−731.

(16) Littler, D. R., Brown, L. J., Breit, S. N., Perrakis, A., and Curmi, P. M. (2010) Structure of human CLIC3 at 2 A resolution. *Proteins 78*, 1594−1600.

(17) Littler, D. R., Assaad, N. N., Harrop, S. J., Brown, L. J., Pankhurst, G. J., Luciani, P., Aguilar, M. I., Mazzanti, M., Berryman, M. A., Breit, S. N., and Curmi, P. M. (2005) Crystal structure of the soluble form of the redox-regulated chloride ion channel protein CLIC4. *FEBS J. 272*, 4996−5007.

(18) Littler, D. R., Harrop, S. J., Brown, L. J., Pankhurst, G. J., Mynott, A. V., Luciani, P., Mandyam, R. A., Mazzanti, M., Tanda, S., Berryman, M. A., Breit, S. N., and Curmi, P. M. (2008) Comparison of vertebrate and invertebrate CLIC proteins: the crystal structures of Caenorhabditis elegans EXC-4 and Drosophila melanogaster DmCLIC. *Proteins 71*, 364−378.

(19) Berryman, M. A., and Goldenring, J. R. (2003) CLIC4 is enriched at cell-cell junctions and colocalizes with AKAP350 at the centrosome and midbody of cultured mammalian cells. *Cell. Motil. Cytoskeleton 56*, 159−172.

(20) Littler, D. R., Harrop, S. J., Fairlie, W. D., Brown, L. J., Pankhurst, G. J., Pankhurst, S., DeMaere, M. Z., Campbell, T. J., Bauskin, A. R., Tonini, R., Mazzanti, M., Breit, S. N., and Curmi, P. M. (2004) The intracellular chloride ion channel protein CLIC1 undergoes a redox-controlled structural transition. *J. Biol. Chem. 279*, 9298−9305.

(21) Singh, H., and Ashley, R. H. (2006) Redox regulation of CLIC1 by cysteine residues associated with the putative channel pore. *Biophys. J. 90*, 1628−1638.

(22) Singh, H., and Ashley, R. H. (2007) CLIC4 (p64H1) and its putative transmembrane domain form poorly selective, redox-regulated ion channels. *Mol. Membr. Biol. 24*, 41−52.

(23) Singh, H., Cousin, M. A., and Ashley, R. H. (2007) Functional reconstitution of mammalian 'chloride intracellular channels' CLIC1, CLIC4 and CLIC5 reveals differential regulation by cytoskeletal actin. *FEBS J. 274*, 6306−6316.

(24) Tulk, B. M., Kapadia, S., and Edwards, J. C. (2002) CLIC1 inserts from the aqueous phase into phospholipid membranes, where it functions as an anion channel. *Am. J. Physiol. Cell. Physiol. 282*, C1103−1112.

(25) Warton, K., Tonini, R., Fairlie, W. D., Matthews, J. M., Valenzuela, S. M., Qiu, M. R., Wu, W. M., Pankhurst, S., Bauskin, A. R., Harrop, S. J., Campbell, T. J., Curmi, P. M., Breit, S. N., and Mazzanti, M. (2002) Recombinant CLIC1 (NCC27) assembles in lipid bilayers

via a pH-dependent two-state process to form chloride ion channels with identical characteristics to those observed in Chinese hamster ovary cells expressing CLIC1. *J. Biol. Chem.* 277, 26003−26011.

(26) Duncan, R. R., Westwood, P. K., Boyd, A., and Ashley, R. H. (1997) Rat brain p64H1, expression of a new member of the p64 chloride channel protein family in endoplasmic reticulum. *J. Biol. Chem.* 272, 23880−23886.

(27) Goodchild, S. C., Howell, M. W., Cordina, N. M., Littler, D. R., Breit, S. N., Curmi, P. M., and Brown, L. J. (2009) Oxidation promotes insertion of the CLIC1 chloride intracellular channel into the membrane. *Eur. Biophys. J.* 39, 129−138.

(28) Tonini, R., Ferroni, A., Valenzuela, S. M., Warton, K., Campbell, T. J., Breit, S. N., and Mazzanti, M. (2000) Functional characterization of the NCC27 nuclear protein in stable transfected CHO-K1 cells. *FASEB J.* 14, 1171−1178.

(29) Fanucchi, S., Adamson, R. J., and Dirr, H. W. (2008) Formation of an unfolding intermediate state of soluble chloride intracellular channel protein CLIC1 at acidic pH. *Biochemistry* 47, 11674−11681.

(30) Stoychev, S. H., Nathaniel, C., Fanucchi, S., Brock, M., Li, S., Asmus, K., Woods, V. L. Jr., and Dirr, H. W. (2009) Structural dynamics of soluble chloride intracellular channel protein CLIC1 examined by amide hydrogen-deuterium exchange mass spectrometry. *Biochemistry* 48, 8413−8421.

(31) Goodchild, S. C., Howell, M. W., Littler, D. R., Mandyam, R. A., Sale, K. L., Mazzanti, M., Breit, S. N., Curmi, P. M., and Brown, L. J. (2010) Metamorphic response of the CLIC1 chloride intracellular ion channel protein upon membrane interaction. *Biochemistry* 49, 5278−5289.

(32) Hudson, E. N., and Weber, G. (1973) Synthesis and characterization of two fluorescent sulfhydryl reagents. *Biochemistry* 12, 4154−4161.

(33) Marsh, D. J., and Lowey, S. (1980) Fluorescence energy transfer in myosin subfragment-1. *Biochemistry* 19, 774−784.

(34) Dewey, T. G., and Datta, M. M. (1989) Determination of the fractal dimension of membrane protein aggregates using fluorescence energy transfer. *Biophys. J.* 56, 415−420.

(35) Corry, B., Rigby, P., Liu, Z. W., and Martinac, B. (2005) Conformational changes involved in MscL channel gating measured using FRET spectroscopy. *Biophys. J.* 89, L49−51.

(36) Corry, B., Jayatilaka, D., and Rigby, P. (2005) A flexible approach to the calculation of resonance energy transfer efficiency between multiple donors and acceptors in complex geometries. *Biophys. J.* 89, 3822−3836.

(37) Majumdar, Z. K., Hickerson, R., Noller, H. F., and Clegg, R. M. (2005) Measurements of internal distance changes of the 30S ribosome using FRET with multiple donor-acceptor pairs: quantitative spectroscopic methods. *J. Mol. Biol.* 351, 1123−1145.

(38) Singh, H. (2010) Two decades with dimorphic Chloride Intracellular Channels (CLICs). *FEBS Lett.* 584, 2112−2121.

(39) Doyle, D. A., Morais Cabral, J., Pfuetzner, R. A., Kuo, A., Gulbis, J. M., Cohen, S. L., Chait, B. T., and MacKinnon, R. (1998) The structure of the potassium channel: molecular basis of K$^+$ conduction and selectivity. *Science* 280, 69−77.

(40) Payandeh, J., Scheuer, T., Zheng, N., and Catterall, W. A. (2011) The crystal structure of a voltage-gated sodium channel. *Nature* 475, 353−358.

(41) Agre, P. (2006) The aquaporin water channels. *Proc. Am. Thorac. Soc.* 3, 5−13.

(42) Fu, D., Libson, A., Miercke, L. J., Weitzman, C., Nollert, P., Krucinski, J., and Stroud, R. M. (2000) Structure of a glycerol-conducting channel and the basis for its selectivity. *Science* 290, 481−486.